

## Effects of Dzyaloshinsky-Moriya Interaction on Planar Rotator Model on Triangular Lattice

Yun-Zhou Sun<sup>1,\*</sup>, Lin Yi<sup>2</sup> and Jian-Sheng Wang<sup>3</sup>

<sup>1</sup> Department of Physics, Wuhan Textile University, Wuhan 430073, China.

<sup>2</sup> Department of Physics, Huazhong University of Science and Technology, Wuhan 430074, China.

<sup>3</sup> Department of Physics, National University of Singapore, Singapore 117542, Singapore.

Received 10 April 2010; Accepted (in revised version) 2 February 2011

Communicated by Michel A. Van Hove

Available online 29 November 2011

---

**Abstract.** The thermodynamic properties and some critical properties of the planar rotator model with chiral Dzyaloshinsky-Moriya (DM) interaction on triangular lattice are analyzed using a hybrid Monte Carlo method. It has been shown that there is a XY-like Berezinskii-Kosterlitz-Thouless (BKT) phase transition in this model. The ground state of this spiral system and the effects of size mismatch are also discussed.

**PACS:** 07.05.Tp, 21.60.Ka, 05.10.Ln, 75.10.Hk

**Key words:** Critical temperature, Dzyaloshinsky-Moriya interaction, Monte-Carlo simulation, vortex.

---

## 1 Introduction

The study of the anisotropic effects on critical behaviors in spin system has attracted much interest. One of the important anisotropies is the so-called Dzyaloshinsky-Moriya (DM) interaction, arising from a mixture of super-exchange and spin-orbit coupling under distorted lattices [1, 2]. It has been shown the DM interaction is responsible for the understanding of the weak ferromagnetism of the low-temperature orthorhombic phase and magnetic structure in copper oxide compound, such as  $\text{La}_2\text{CuO}_4$  and some Fe and Cr jarosites [3–8]. The DM interactions play an important role in the study of spin glasses as well as the explanation of some neutron scattering measurements [9, 10]. Due to the

---

\*Corresponding author. Email addresses: syz1979@163.com (Y.-Z. Sun), yilin@mail.hust.edu.cn (L. Yi), phywjs@nus.edu.sg (J.-S. Wang)

lack of centrosymmetry of the lattice, the DM interaction can induce a helical chiral magnetic order [11–15]. Recently, it is found that DM interaction is the primary source of anisotropy and plays an important role for understanding of the magnetization and spin structure in antiferromagnetic materials [16]. The effects of DM interactions on low energy magnetic excitations have also investigated extensively by spin wave analysis and direct numeric simulations [17–19]. The study of classical and quantum XY model with DM interactions on a triangular lattice by real space renormalization group method and spin molecular dynamics simulations indicated that the Berezinskii-Kosterlitz-Thouless (BKT) phase could appear at low temperatures [20]. Wilson renormalization group results showed that adding DM interactions on the classical ferromagnetic Heisenberg model, there exists a XY-like phase transition [21]. In addition, Monte-Carlo (MC) simulations and self-consistent harmonic approximation theory were also used to calculate the BKT transition for the two-dimensional classical Heisenberg model with DM interaction [22, 23]. To the best of our knowledge, the most of numeric simulations have been focused on the study of strong DM interactions for antiferromagnetic spin models. On appearance of anisotropic interactions, however, the spin system may display complex thermodynamic and magnetic characteristics due to the competition between spin coupling and DM interactions. In this work, we adopt a hybrid Monte-Carlo method to study the effects of the DM term on planar rotator model on triangular lattices.

## 2 Model and simulation method

The Hamiltonian of the classical spin planar rotator model with a DM interaction term between spins can be written as [20, 24, 25]

$$H = -J \sum_{\langle ij \rangle} \vec{S}_i \cdot \vec{S}_j - \sum_{\langle ij \rangle} \vec{D} \cdot (\vec{S}_i \times \vec{S}_j). \quad (2.1)$$

Here  $J = 1$  is the reduced ferromagnetic coupling constant,  $\theta_i$  are the angular coordinates of two-component spins  $\vec{S}_i = (S_i^x, S_i^y) = (\cos\theta_i, \sin\theta_i)$  and  $i, j$  indicate the nearest neighbor sites of a triangular lattice. For the application of a cluster algorithm, Eq. (2.1) can be simplified into

$$H = -\tilde{J} \sum_{\langle ij \rangle} \cos(\theta_i - \theta_j - \varphi). \quad (2.2)$$

By considering the direction of DM interaction vector  $\vec{D} = D\hat{z}$  along the positive  $z$ -axial direction. For simplicity,  $\tilde{J} = J\sqrt{1+d^2}$ ,  $d = D/J$  and  $\varphi = \tan^{-1}(J/\tilde{J})$ . Note that when  $d = \sqrt{3}$ , namely  $\varphi = \pi/3$ , this model coincides with the fully frustrated XY model if the sum of  $\varphi$  along an elementary triangular cell is equal to  $\pi$  [26, 27].

In order to prevent critical slowing down and correlations for different configurations, we use a hybrid MC method, including cluster and single spin updates to calculate the thermodynamic quantities for the model Hamiltonian Eq. (2.2). The simulations consist

of one Swendsen-Wang (SW) cluster update [28, 29] followed by one Metropolis single spin update in each MC step [30]. In an SW update process, we introduce a transformation  $\theta_i \rightarrow \theta_i + \frac{1-\sigma_i}{2}\pi$ . Eq. (2.2) can be rewritten as

$$H = -\tilde{J} \sum_{\langle i,j \rangle} \cos\left(\theta_i - \theta_j + \frac{1-\sigma_i}{2}\pi + \frac{1-\sigma_j}{2}\pi - \varphi\right) = -\tilde{J} \sum_{\langle i,j \rangle} \cos(\theta_i - \theta_j - \varphi) \sigma_i \sigma_j,$$

where  $\sigma_i = \pm 1$ . Now we define an effective Ising coupling  $H_{\text{Ising}} = -\sum_{i,j} J_{ij} \sigma_i \sigma_j$ , where  $J_{ij} = -\tilde{J} \cos(\theta_i - \theta_j - \varphi)$ . If  $J_{ij} \sigma_i \sigma_j > 0$ , we put a bond between two nearest spins with probability

$$p = 1 - e^{-2J_{ij} \sigma_i \sigma_j / k_B T}.$$

Otherwise, there is no need to put bond between the nearest spins. In the next step, a Hoshen-Kopelman method is used to identify all clusters of sites which are produced by a connected network of bonds. In the following, one cluster is chosen to be updated with probability 1/2 and a new spin arrangement is formed. In our simulation,  $10^4$  MC steps were discarded for thermal equilibration. about  $5 \times 10^5$  MC steps were used to get thermal averages.

### 3 Results and discussions

We first discuss the ground state of this model. DM interaction can make the spin to arrange in a canted degree with its nearest neighbors [14, 32]. Fig. 1 shows a typical ground state spin configuration with DM interaction. Here we assume that the DM vector is along two opposite direction.  $d > 0$  means the positive z-axial direction and  $d < 0$  means negative z-axial direction. It is noted that the magnetic spin has a spiral periodic arrangement. The periodicity is independent of the direction of the DM interaction vector, but dependent on the magnitude of  $d$ . By changing the sign of  $d$ , based on the definition of  $\varphi$ , the sign of  $\varphi$  in Eq. (2.2) is altered too. Since  $\varphi$  means the average difference of an elementary triangle of the lattice on the ground state, the angular displacement between nearest neighbor rotors changes sign as the sign of  $\varphi$  is changed. That is to say, the orientation of the DM vector only effects the spin arrangement direction, as shown by the arrows in Fig. 1(b)-(c). From Fig. 1(b)-(c), one notices that the spins along the horizontal bonds undergo a complete  $2\pi$  rotation over 10 lattice constants while along the two other directions of the triangular lattice, 20 lattice constants are needed to perform a full  $2\pi$  rotation. With some fluctuations the nearest neighbor phase differences are about  $2\pi/10$  and  $2\pi/20$  respectively. Each triangular plaquette in the ground state has the similar spin configuration as illustrated in Fig. 2. For the orientation of bonds defined as the red arrows in Fig. 2, the energy per plaquette can be written as

$$U = -\tilde{J} [\cos(\alpha_1 - \varphi) + \cos(\alpha_2 - \varphi) + \cos(\alpha_3 - \varphi)], \quad (3.1)$$

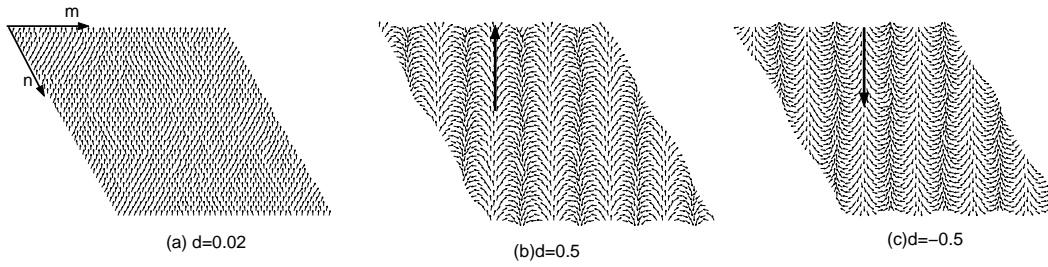


Figure 1: Spin configurations of ground state for different DM interactions (a)  $d=0.02$ , (b)  $d=0.5$ , (c)  $d=-0.5$ . The temperature of simulation is  $T=0.05$ .

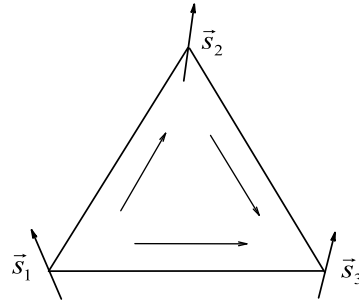


Figure 2: Example of a unit plaquette of ground state in triangular lattice. The arrows in the triangle indicate the orientations of bonds.

where  $\alpha_1 = \theta_1 - \theta_2$ ,  $\alpha_2 = \theta_2 - \theta_3$  and  $\alpha_3 = \theta_1 - \theta_3 = \alpha_1 + \alpha_2$  are the phase differences along the orientations of bonds. We minimize the energy for both  $\alpha_1$  and  $\alpha_2$ ,  $\partial U / \partial \alpha_1 = \partial U / \partial \alpha_2 = 0$ , that is

$$\sin(\alpha_1 - \varphi) + \sin(\alpha_1 + \alpha_2 - \varphi) = \sin(\alpha_2 - \varphi) + \sin(\alpha_1 + \alpha_2 - \varphi) = 0.$$

Then we obtain the result  $\alpha_1 = \alpha_2 = \Delta\theta$ , which indicates that the nearest neighbors phase differences  $\Delta\theta$  on the non-horizontal bonds are all the same. The relation of ground state phase difference and parameter  $d$  can be written as follows

$$d = \tan(\varphi) = \tan\left(\frac{3}{2}\Delta\theta\right). \quad (3.2)$$

We can get the ground state phase difference of nearest spins for any given value of  $d$ . For example, at  $d=0.5$ , Eq. (3.2) gives  $\Delta\theta = 0.309 \approx \pi/10$ , in excellent agreement with the angles measured in Fig. 1. Then the periodicity  $Q$  of spin arrangements on ground state can be obtained for any given values of  $d$ . The incommensurability of the ground state periodicity with the finite lattice size and the boundary conditions may have a significant effect on the thermodynamic quantities and the nature of phase transition [32–35]. When the system is incommensurate, periodic boundary conditions will serve to introduce "frustration" and act as an external stress in all space directions [32, 34]. In the following, we discuss the effects of this mismatch on the thermodynamic quantities and critical properties.

Usually, the magnetization is used as an order parameter in the Monte Carlo simulations for XY model. Here the spin arrangement is not parallel at ground state because of DM interaction. Therefore, according to the spin configuration of this model, we define a new order parameter as

$$M = \sqrt{(M_x)^2 + (M_y)^2} = \sqrt{\left(\sum_{i=1}^N \cos[\theta_i + (m+2n)\Delta\theta]\right)^2 + \left(\sum_{i=1}^N \sin[\theta_i + (m+2n)\Delta\theta]\right)^2}, \quad (3.3)$$

where  $m, n \in [0, L-1]$  are integers and indicate the location of spin, as shown in Fig. 1.  $M_x$  and  $M_y$  are the order parameter components of  $x$  direction and  $y$  direction. As the MC proceeds, we record the time series of the energy density  $e = E/N$ , where lattice size  $N = L \times L$ . For each temperature, some thermodynamic quantities are observed [25,31]

$$\chi^\alpha = \frac{[\langle (M_\alpha)^2 \rangle - \langle M_\alpha \rangle^2]}{Nk_B T}, \quad (3.4a)$$

$$\chi' = \frac{(\chi^x + \chi^y)}{2}, \quad (3.4b)$$

$$C_V = \frac{[\langle E^2 \rangle - \langle E \rangle^2]}{Nk_B T^2}, \quad (3.4c)$$

where  $\chi_\alpha$  is the order parameter susceptibility component ( $\alpha$  can be taken as  $x$  or  $y$  component in 2D model),  $\chi'$  is the in-plane order parameter susceptibility,  $C_V$  is the specific heat and  $T$  denotes temperature.

In this paper, the temperature, the specific heat, the energy per spin, the order parameter and the in-plane order parameter susceptibility are measured in unites of  $J/k_B$ ,  $k_B$ ,  $J$ ,  $S$  and  $(S)^2$ , respectively. Here  $k_B$  is the Boltzmann constant. The spin length  $S = 1$  is used for simplicity. In the presenting figures, the statistical errors are smaller than the symbol sizes.

Physically, any long-range order which otherwise would be present is destroyed by spin wave excitations in planar rotator spin models. The existence of a phase with conventional long range order at any non zero temperature is precluded by the Mermin-Wagner theorem [36]. Therefore there is no spontaneous magnetization in two-dimensional spin models. In such models there can however exist topological long range order. Kosterlitz and Thouless used approximate renormalization group method to demonstrate that this transition is caused by the unbinding of vortex-antivortex pairs [37, 38]. The scenario is that at temperatures above some critical value  $T_c$  the vortices and anti-vortices are unbounded and serve to disorder the system. Decreasing the temperature causes the vortices and anti-vortices to bind. Then the phase transition exhibits some essential scaling behavior, such as the order parameter susceptibility scales with a power of the lattice size,  $\chi' \propto L^{2-\eta}$ , where theoretically the critical exponent  $\eta$  is  $1/4$  at the phase transition temperature. The DM interaction can induce an easy-plane anisotropy, from which a BKT type transition has been expected in a two-dimensional classical Heisenberg model with a DM interaction [22]. Due to both the absence of spectacular peaks and a logarithmic correction that gives problems with ordinary finite-size

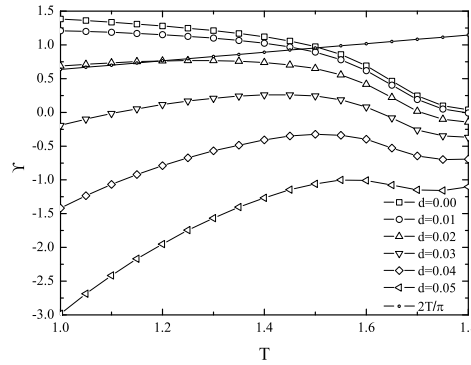


Figure 3: Helicity modulus as a function of  $T$  for different  $d$  values at the fixed size  $L=48$ .

scaling, the precise determination of the temperature for a BKT transition is a difficult task. The helicity modulus,  $Y$ , obtained by a measure of the resistance to an infinitesimal spin twist  $\Delta$  across the system along one coordinate, is a good way to show a BKT transition. For a model Hamiltonian,  $Y$  takes the generic expression [39, 40]

$$Y = \frac{\langle \frac{\partial^2 H}{\partial \Delta^2} \rangle}{N} - \beta \frac{\langle (\frac{\partial H}{\partial \Delta})^2 \rangle - \langle \frac{\partial H}{\partial \Delta} \rangle^2}{N}, \tag{3.5}$$

where  $\beta = (k_B T)^{-1}$  is the inverse temperature. For the planar rotator model with a DM interaction, defined by Eq. (2.2), based on the derivation process of [41], we can get the expression of helicity modulus on the triangular lattice

$$Y(T) = -\frac{\langle H \rangle}{\sqrt{3}} - \frac{2\tilde{J}^2}{\sqrt{3}k_B T N^2} \left\langle \left[ \sum_{\langle i,j \rangle} (\hat{e}_{ij} \cdot \hat{x}) \sin(\theta_i - \theta_j - \varphi) \right]^2 \right\rangle. \tag{3.6}$$

Here  $\hat{e}_{ij}$  is the unit vector pointing from site  $j$  to site  $i$ .  $\hat{x}$  is a selected basis vector in one coordinate. There are universal relations between the helicity modulus and the critical temperature, which are like fingerprints for the BKT transition. According to the renormalization group theory [37], critical temperature can be estimated from the intersection of the helicity modulus  $Y(T)$  and the straight line  $Y = 2k_B T / \pi$ . The MC data of  $Y(T)$  will have a deeper drop in the critical region with increase of lattice size. For larger lattice size, the intersection will be nearer to the critical temperature. Therefore, an over-estimate of  $T_c$  may be obtained by this method. We first consider the case that the DM interaction is small,  $d < 0.1$ .

Fig. 3 shows the results of different  $d$  for fixed system size  $L = 48$ , which is smaller than the periodicity of spin arrangement. It is clear that there is a crossing point for  $d < 0.03$ . The intersections disappear for  $d > 0.03$ . For  $d = 0.00$ , as an example, the transition temperature is  $T_c \approx 1.50$ . This data is comparable with the result of high temperature expansions [42, 43]. It is noted that the helicity modulus has a negative value when  $d \geq 0.03$ . The negative value indicates that there is a lower free energy than the unperturbed

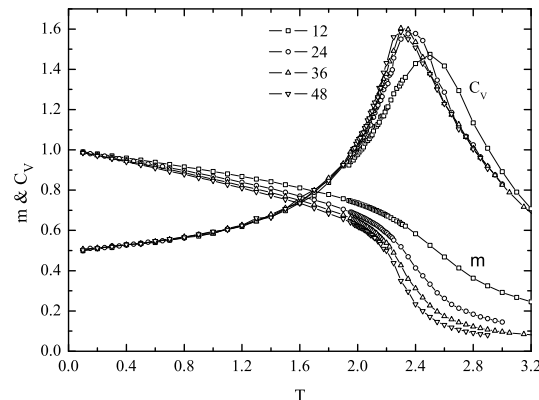


Figure 4: Order parameter and specific heat for different lattice sizes at fixed  $d=1.0$ , where  $m=M/N$  is order parameter density.

energy in a twisted system. This is due to the fact that Eqs. (3.5) and (3.6) are constructed for periodic boundary conditions and the system sizes are limited in one periodicity of spin arrangement. So the spins on the boundary line have a mismatch with its nearest neighbors. This mismatch affects the value of helicity modulus using Eq. (3.5), which is derived from periodic boundary conditions.

Meanwhile, periodic boundary conditions generally cause a mismatch around critical temperature causing an artificial "stress" on the spin structure. This could have a significant effect on the nature of the phase, especially when the system size is not large enough compared with the periodicity [33]. Then a type of spiral phase transition whose spin structure is typically incommensurate occurs at finite temperature. In this case, the ground state structure will be governed mainly by the DM interaction, just as shown in Fig. 1(b)-(c). This spiral phase is expected to be a XY-like BKT transition [21]. The minimum periodic length required to fully accommodate the ground state structure in the short periodicity bond direction is given by  $Q = \pi / \Delta\theta$ . For example, for  $d=0.05$  we have  $Q \approx 94$ . In the thermodynamic limit, the order parameter will be always finite and close to 1, as shown in Fig. 4. The specific heat is also shown in Fig. 4. If the lattice size is incommensurate with the periodicity, the order parameter will collapse at the low temperature, for example in some helimagnets. To avoid this mismatch, one approach is to employ free boundary conditions and take very large lattice size to eliminate surface effects. But this will need more time to attain the data. Another approach of trying to commensurate the size mismatch would be to take the system size as an integral multiple of one periodicity length. Thus the boundary will be suitable for this system and some methods based on period boundary conditions can also be used directly. For example, for  $d=1.0$  we can have  $Q=6$ , which is just an integer. Fig. 5 shows the helicity modulus obtained from Eq. (3.6), where the system sizes are taken as  $L=12, 24, 36$  and  $48$ . The MC data indicate the helicity modulus is positive at all temperatures. With the increased lattice sizes, a deep drop appears near the temperature of the peak of specific heat. From the

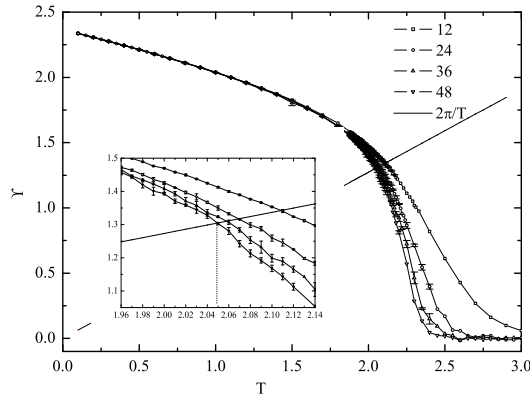


Figure 5: Helicity modulus as a function of  $T$  for different lattice sizes at the fixed DM interaction  $d=1.0$ .

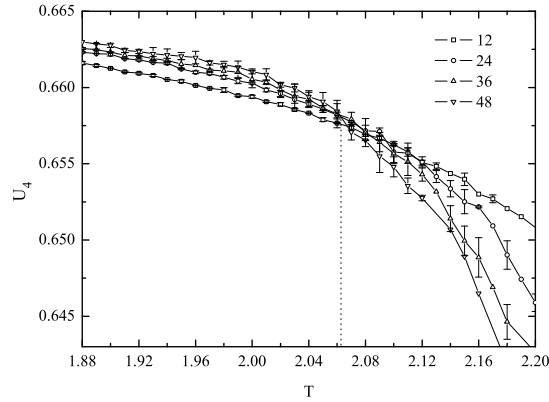


Figure 6: Application of Binders fourth order cumulant to estimate the phase transition temperature for several lattice sizes at  $d=1.0$ .

crossing point of  $Y(T)$  and the straight line  $Y = 2k_B T / \pi$  for the largest size  $L = 48$ , the phase transition temperature is estimated at about  $T_C = 2.05$ .

Another approach called Binder’s fourth-order cumulant can be used to estimate the location of  $T_C$  in the thermodynamic limit. The Binder’s fourth order cumulant can be defined as

$$U_L = 1 - \frac{\langle M^4 \rangle}{3 \langle M^2 \rangle^2}. \tag{3.7}$$

At the phase transition temperature,  $U_L$  is expected to be approximately independent of the system size. Therefore,  $T_C$  can be obtained from the crossing point of  $U_L$  for different lattice sizes. As an example, Fig. 6 shows  $U_L$  for different lattice sizes at  $d=1.0$ . The phase transition temperature is estimated at about  $T_C = 2.06$ . Generally speaking, this method overestimates  $T_C$ . With increasing  $L$ , the estimation of  $T_C$  will be more accurate. Due to the statistical uncertainties, however, more computer time is required to calculate near  $T_C$ .

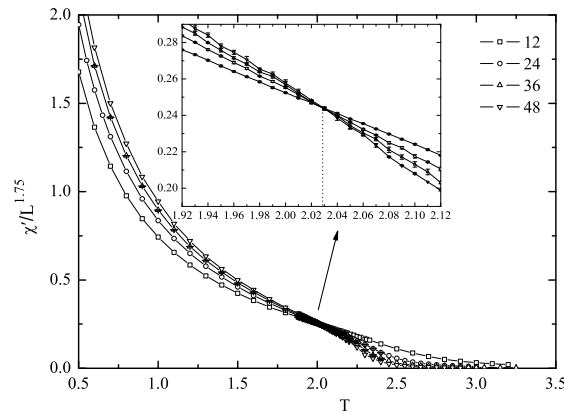


Figure 7: Application of the finite-size scaling of in-plane order parameter susceptibility to estimate the phase transition temperature.

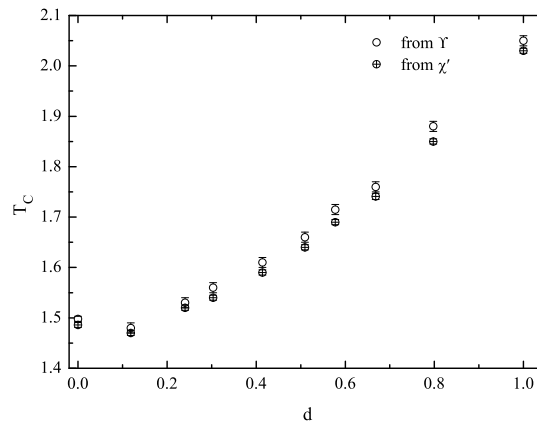


Figure 8: Phase transition temperature for different DM interactions.

Theoretically, the critical exponent  $\eta$  is  $1/4$  at the BKT phase transition point. From the finite size scaling analysis of the in-plane order parameter susceptibility, near and below  $T_C$ , the order parameter susceptibility scales with a power of the lattice size,  $\chi' \propto L^{2-\eta}$ . Therefore, using  $\eta = 1/4$ , from the common point of intersection of the curves  $\chi'/L^{7/4}$  vs  $T$ , the phase transition temperature can be obtained [44–46]. Fig. 7 shows the application of this method at  $d = 1.0$ . The estimation of  $T_C$  is about 2.03, which is very close to the result of helicity modulus method. From the scaling relation, we can get  $\eta = 0.26$  at  $T = 2.05$ , very close to the theoretical value. Both the results of the helicity modulus and critical exponent have shown that the phase transition of this model is a BKT type. Using the methods above, the phase transition temperature at different DM interactions is shown in Fig. 8. Obviously,  $T_C$  increases with the DM interaction.

The scenario of the BKT phase transition shows topological long-range order exists in the system at low temperature and the vortex and antivortex are bounded as pairs. How-

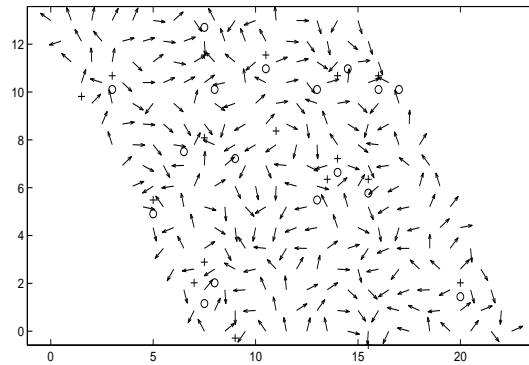


Figure 9: Plot of spin configuration at  $T=2.1$ ,  $d=1.0$ . The sign "+" indicates the positive vortex and "O" indicates the negative vortex.

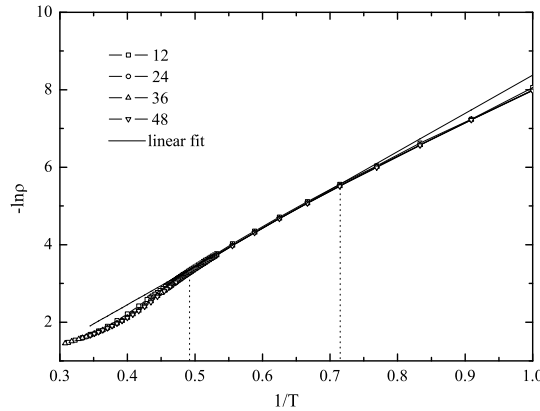


Figure 10: Log of vortex density as a function of  $1/T$  for different lattice sizes. The solid straight line is the linear fitted line to the low temperature data. The dotted lines indicate the fitted region of temperature.

ever, the number of vortices proliferates at high temperature. Meanwhile, the distance between vortex-antivortex pairs becomes so large that they are effectively free and render the system disordered. Fig. 9 shows a snapshot of unbinding of vortex and antivortex at  $T=2.1$ , just above the critical temperature. In order to get the vortex density, we simulate with different lattices under periodic boundary conditions. According to the BKT theory, the vorticity  $q$  is defined as follows [37,38],

$$q = \frac{1}{2\pi} \oint d\theta(r), \tag{3.8}$$

where  $\theta(r)$  is the angle which a spin situated at  $r$  with the fixed axis. The integral is taken round the boundary in each elementary triangle plaquette consisting of three spins at the corners. The vortex density  $\rho$  is defined as the total number of vortex (positive vortex and negative vortex) divided by the number of spins. In the limit,  $\rho$  is expected as a exponential dependence with the energy  $2\mu$  which is the contribution of creating a

vortex-antivortex pair,  $\rho \sim e^{-2\mu/T}$ . The theoretical value of  $2\mu$  is 10.2 in the BKT prediction [47]. In order to get the result of  $2\mu$ , we plot  $-\ln\rho$  as the function of  $1/T$  in Fig. 10. To be compared with the theoretical value, in the low temperature region of  $T$  at  $1.4 \sim T_C$ , we estimate  $2\mu = 9.80$  using a linear fit. Above  $T_C$ , vortex density increases and  $2\mu$  decreases as the temperature increases, which indicates that it is easier to generate more vortices when many vortices are already present disordering the spins.

## 4 Conclusions

In conclusions, with an improved Swendsen-Wang algorithm, we studied the effects of the DM term of a planar rotator model on the thermodynamic properties and some critical properties as well as the spin magnetic structure on a triangular lattice. It was found that there is an XY-like BKT transition in this model with DM interaction. On the other hand, we studied the ground state of system and verified that the periodicity of spin arrangements only depends on the strength of the DM interaction. Meanwhile, we define an efficient order parameter to describe the configuration. Moreover, the thermodynamics quantities are independent of spin arrangements because of the symmetry of the Hamiltonian equation. The effects of the size mismatch on the thermodynamic quantities are also discussed. We explain the reasons of negative value of the helicity modulus and give one approach to solve this problem. In addition, the phase transition temperatures are obtained by different methods and the properties of vortex density are also discussed.

## Acknowledgments

This work was supported by the Youth Foundation of Hubei Provincial Department of Education under Grant No. Q20101602 and the Foundation of Wuhan Textile University. Sun also thanks the anonymous referees for their useful discussions and comments.

## References

- [1] I. E. Dzyaloshinskii, A thermodynamic theory of "weak" ferromagnetism of antiferromagnetics, *J. Phys. Chem. Solids*, 4 (1958), 241–255.
- [2] T. Moriya, New mechanism of anisotropic superexchange interaction, *Phys. Rev. Lett.*, 4 (1960), 228–230.
- [3] A. S. Wills, Long-range ordering and representational analysis of the jarosites, *Phys. Rev. B*, 63 (2001), 064430–064443.
- [4] T. Inami, T. Morimoto, M. Nishiyama, S. Maegawa, Y. Oka and H. Okumura, Magnetic ordering in the kagomé lattice antiferromagnet  $\text{KCr}_3(\text{OD})_6(\text{SO}_4)_2$ , *Phys. Rev. B*, 64 (2001), 054421–054427.
- [5] A. S. Wills, A. Harrison, C. Ritter and R. I. Smith, Magnetic properties of pure and diamagnetically doped jarosites: model kagomé antiferromagnets with variable coverage of the magnetic lattice, *Phys. Rev. B*, 61 (2000), 6156–6169.

- [6] T. Inami, M. Nishiyama, S. Maegawa and Y. Oka, Magnetic structure of the kagomé lattice antiferromagnet potassium jarosite  $\text{KFe}_3(\text{OH})_6(\text{SO}_4)_2$ , *Phys. Rev. B*, 61 (2000), 12181–12186.
- [7] W. Koshibae, Y. Ohta and S. Maekawa, Electronic and magnetic structures of cuprates with spin-orbit interaction, *Phys. Rev. B*, 47 (1993), 3391–3400.
- [8] M. Elhajal, B. Canals and C. Lacroix, Ordering in pyrochlore compounds due to Dzyaloshinsky-Moriya interactions: the case of  $\text{Cu}_4\text{O}_3$ , *J. Phys. Condens. Matter*, 16 (2004), S917–S922.
- [9] L. Yi, G. Buttner, K. D. Usadel and K. L. Yao, Quantum Heisenberg spin glass with Dzyaloshinskii-Moriya interactions, *Phys. Rev. B*, 47 (1993), 254–261.
- [10] F. Coomer, A. Harrison, G. S. Oakley, J. Kulda, J. R. Stewart, J. A. Stride, B. Fak, J. W. Taylor and D. Visser, Inelastic neutron scattering study of magnetic excitations in the kagome antiferromagnet potassium jarosite, *J. Phys. Condens. Matter*, 18 (2006), 8847–8855.
- [11] P. Bak and M. H. Jensen, Theory of helical magnetic structures and phase transitions in MnSi and FeGe, *J. Phys. C*, 13 (1980), L881–L887.
- [12] O. Nakanishi, A. Yanase, A. Hasegawa and M. Kataoka, The origin of the helical spin density wave in MnSi, *Solid State Commun.*, 35 (1980), 995–998.
- [13] M. Uchida, Y. Onose, Y. Matsui and Y. Tokura, Real-space observation of helical spin order, *Science*, 311 (2006), 359–361.
- [14] E. Y. Vedmedenko, L. Udvardi, P. Weinberger and R. Wiesendanger, Chiral magnetic ordering in two-dimensional ferromagnets with competing Dzyaloshinsky-Moriya interactions, *Phys. Rev. B*, 75 (2007), 104431–104439.
- [15] M. Elhajal, B. Canals and C. Lacroix, Symmetry breaking due to Dzyaloshinsky-Moriya interactions in the kagomé lattice, *Phys. Rev. B*, 66 (2002), 014422–014428.
- [16] T. Yildirim and A. B. Harris, Magnetic structure and spin waves in the Kagomé jarosite compound  $\text{KFe}_3(\text{SO}_4)_2(\text{OH})_6$ , *Phys. Rev. B*, 73 (2006), 214446–214470.
- [17] K. Matan, D. Grohol, D. G. Nocera, T. Yildirim, A. B. Harris, S. H. Lee, S. E. Nagler and Y. S. Lee, Spin waves in the frustrated Kagomé lattice antiferromagnet  $\text{KFe}_3(\text{OH})_6(\text{SO}_4)_2$ , *Phys. Rev. Lett.*, 96 (2006), 247201–247205.
- [18] A. Benyoussef, A. Boubekri and H. Ez-Zahraouy, Spin-wave analysis of the XXZ Heisenberg model with Dzyaloshinskii-Moriya interaction, *Phys. B*, 266 (1999), 382–390.
- [19] J. Z. Zhao, X. Q. Wang, T. Xiang, Z. B. Su and L. Yu, Effects of the Dzyaloshinskii-Moriya interaction on low-energy magnetic excitations in copper Benzoate, *Phys. Rev. Lett.*, 90 (2003), 207204–207208.
- [20] L. Biegala, A. Drzewiński and J. Sznajd, Low temperature phase of the quantum triangular lattice XY model with Dzyaloshinsky-Moriya interaction, *Phys. A*, 225 (1996), 254–270.
- [21] L. L. Liu, Physics has changed, *Phys. Rev. Lett.*, 13 (1973), 459–460.
- [22] A. S. T. Pires, Kosterlitz-Thouless transition in the Heisenberg model with antisymmetric exchange interaction, *Solid State Commun.*, 112 (1999), 705–706.
- [23] K. W. Lee and C. E. Lee, Monte Carlo study of the Kosterlitz-Thouless transition in the Heisenberg model with antisymmetric exchange interactions, *Phys. Rev. B*, 72 (2005), 054439–054445.
- [24] Y. Z. Sun, H. P. Liu and L. Yi, Monte Carlo study of planar rotator model with weak Dzyaloshinsky-Moriya interaction, *Commun. Theor. Phys.*, 46 (2006), 663–667.
- [25] H. P. Liu, Y. Z. Sun and L. Yi, New Monte Carlo simulations to a generalized XY model, *Chin. Phys. Lett.*, 23 (2006), 316–319.
- [26] G. Franzese, V. Cataudella, S. E. Korshunov and R. Fazio, Fully frustrated XY model with next-nearest-neighbor interaction, *Phys. Rev. B*, 62 (2000), R9287–R9290.

- [27] S. E. Korshunov, Kink pairs unbinding on domain walls and the sequence of phase transitions in fully frustrated XY models, *Phys. Rev. Lett.*, 88 (2002), 167007–167011.
- [28] J.-S. Wang and R. H. Swendsen, Cluster Monte Carlo algorithms, *Phys. A*, 167 (1990), 565–579.
- [29] R. H. Swendsen and J.-S. Wang, Nonuniversal critical dynamics in Monte Carlo simulations, *Phys. Rev. Lett.*, 58 (1987), 86–88.
- [30] N. Metropolis, A. W. Rosenbluth, M. N. Rosenbluth, A. H. Teller and E. Teller, Equation of state calculation by fast computing machines, *J. Chem. Phys.*, 21 (1953), 1087–1092.
- [31] E. Rastelli, S. Regina and A. Tassi, Monte Carlo simulation for square planar model with a small fourfold symmetry-breaking field, *Phys. Rev. B*, 70 (2004), 174447–174452.
- [32] H. Kawamura, Universality of phase transitions of frustrated antiferromagnets, *J. Phys. Cond. Matter*, 10 (1998), 4707–4754.
- [33] H. Kawamura, Critical properties of helical magnets and triangular antiferromagnets, *J. Appl. Phys.*, 63 (1988), 3086–3098.
- [34] W. M. Saslow, M. Gabay and W.-M. Zhang, “Spiraling” algorithm: collective Monte Carlo trial and self-determined boundary conditions for incommensurate spin systems, *Phys. Rev. Lett.*, 68 (1992), 3627–3630.
- [35] H. T. Diep, Magnetic transitions in helimagnets, *Phys. Rev. B*, 39 (1989), 397–404.
- [36] N. D. Mermin and H. Wagner, Absence of Ferromagnetism or Antiferromagnetism in one- or two-dimensional isotropic Heisenberg models, *Phys. Rev. Lett.*, 17 (1966), 1133–1136.
- [37] J. M. Kosterlitz and D. J. Thouless, Ordering, metastability and phase transitions in two-dimensional systems, *J. Phys. C*, 6 (1973), 1181–1191.
- [38] J. M. Kosterlitz, The critical properties of the two-dimensional XY model, *J. Phys. C*, 7 (1974), 1046–1152.
- [39] G. Ramirez-Santiago and J. V. Jose, Critical exponents of the fully frustrated two-dimensional XY model, *Phys. Rev. B*, 49 (1994), 9567–9582.
- [40] H. Weber and P. Minnhagen, Monte Carlo determination of the critical temperature for the two-dimensional XY model, *Phys. Rev. B*, 37 (1988), 5986–5989.
- [41] D. H. Lee, J. D. Joannopoulos, J. W. Negele and D. P. Landau, Symmetry analysis and Monte Carlo study of a frustrated antiferromagnetic planar (XY) model in two dimensions, *Phys. Rev. B*, 33 (1986), 450–475.
- [42] P. Butera and M. Comi, High-temperature study of the Kosterlitz-Thouless phase transition in the XY model on the triangular lattice, *Phys. Rev. B*, 50 (1994), 3052–3057.
- [43] M. Campostrini, A. Pelissetto, P. Rossi and E. Vicari, Strong-coupling analysis of two-dimensional  $\mathcal{O}(N)\sigma$  models with  $N \leq 2$  on square, triangular and honeycomb lattices, *Phys. Rev. B*, 54 (1996), 7301–7317.
- [44] A. Cuccoli, V. Tognetti and R. Vaia, Two-dimensional XXZ model on a square lattice: a Monte Carlo simulation, *Phys. Rev. B*, 52 (1995), 10221–10231.
- [45] G. M. Wysin and A. R. Bishop, Dynamic correlations in a classical two-dimensional Heisenberg antiferromagnet, *Phys. Rev. B*, 42 (1990), 810–819.
- [46] G. M. Wysin, Vacancy effects in an easy-plane Heisenberg model: reduction of  $T_c$  and doubly charged vortices, *Phys. Rev. B*, 71 (2005), 094423–094434.
- [47] R. Gupta and C. F. Baillie, Critical behavior of the two-dimensional XY model, *Phys. Rev. B*, 45 (1992), 2883–2898.